

**EFFECT OF ELECTROLESS PLATING ON WEAR AND  
SURFACE FRICTION OF AISi CYLINDER LINER**

**by**

**MUKRIDZ BIN MD MOHTAR**

**Thesis submitted in fulfilment of the requirements**

**for the degree of**

**Master of Science**

**July 2012**

## DECLARATION

I hereby declare that the work reported in this thesis is the result of my own investigation and that no part of the thesis has been plagiarized from external sources. Materials taken from other sources are duly acknowledged by giving explicit references.

Signature: .....

Name of student: MUKRIDZ BIN MD MOHTAR

Matrix number: P-CM0310

Date: .....

## **ACKNOWLEDGEMENT**

**Praise and thanks are due to Almighty Allah,  
the Most Gracious the Most Merciful**

I would like to express my truly gratitude and highest appreciation to my supervisors, Assoc. Prof. Dr. Zaidi bin Mohd Ripin and Prof. Dr. Haji Zainal Arifin bin Ahmad, for their precious guidance, support, training, advice and encouragement throughout my study. Without them, this research will not be the same as presented here. I also would like to thank all the technicians especially Mr. Wan Mohd Amri bin Wan Mamat Ali, Mr. Mohd Ashamuddin bin Hashim, Mr. Baharom bin Awang, Mr. Azhar bin Ahmad and Mr. Mohamad Zaini bin Saari, for their valuable support and help. Apart of that, I want to thank to all my fellow friends from the Vibration Lab whose give their help, moral support, and some valuable hints for completing my research.

Besides that, I am gratitude to Kementerian Pengajian Tinggi Malaysia and Universiti Malaysia Perlis for awarding me Skim Latihan Akademik Bumiputera (SLAB) scholarship which assisted my financial.

Last but not least, I would like to express my deepest gratitude to my parent, my wife, Dr. Norsamihah binti Haji Ramli, my children and my whole family for their kindly love and continuous support during my intricate times in completing this research. A truly thankfulness are dedicated to all who involve in this project directly and indirectly. Thank you very much.

MUKRIDZ BIN MD MOHTAR

July 2012

## TABLE OF CONTENTS

DECLARATION .....	ii
ACKNOWLEDGEMENT .....	iii
TABLE OF CONTENTS .....	iv
LIST OF TABLES .....	viii
LIST OF FIGURES .....	ix
NOMENCLATURE.....	xv
ABSTRAK .....	xx
ABSTRACT.....	xxii
CHAPTER ONE INTRODUCTION .....	1
1.1 Background.....	1
1.2 Problem statement.....	2
1.3 Research objective .....	3
1.4 Scope of research .....	3
1.5 Thesis outline.....	4
CHAPTER TWO LITERATURE REVIEW.....	5
2.1 Overview.....	5
2.2 Tribological performance study of piston assembly.....	5
2.3 Maximum temperature at TDC of an IC engine .....	17
2.4 Lubrication.....	18

2.4.1	Lubrication regime and Stribeck curve .....	18
2.4.2	Lubrication performance studies.....	20
2.5	Coating on AlSi -alloy cylinder bore .....	22
2.6	Electroless nickel plating .....	25
2.7	Discussion .....	29
2.8	Summary .....	32
CHAPTER THREE METHODOLOGY.....		33
3.1	Introduction.....	33
3.2	Wear-test rig design and fabrication .....	33
3.3	Wear experiment setting and procedure .....	38
3.3.1	Measurement of the piston ring tension .....	43
3.3.2	Specimens hardness against temperature difference.....	43
3.4	Surface characterisation .....	44
3.4.1	Non-contact Metrology .....	44
3.4.2	Average roughness ( $R_a$ ) .....	45
3.4.3	Bearing ratio curve.....	46
3.5	Wear analysis .....	48
3.5.1	Wear volume .....	48
3.5.2	Wear depth .....	50
3.5.3	Four-Ball wear test.....	51
3.6	Electroless Ni-P-C <sub>g</sub> -SiC coating.....	54

3.6.1	Pretreatment of AlSi-alloy substrate .....	54
3.6.2	Plating set up .....	56
3.6.3	Post treatment after coating process.....	59
3.6.4	Vickers micro hardness test .....	60
3.6.5	SEM and EDX .....	60
3.6.6	X-Ray diffraction .....	61
3.7	Summary .....	62
CHAPTER FOUR RESULTS AND DISCUSSION.....		64
4.1	Overview .....	64
4.2	The piston ring tension.....	64
4.3	Electroless Ni-P-C <sub>g</sub> -SiC composite coating characterisation .....	65
4.4	Hardness of AlSi-alloy liner and piston ring at different temperature.....	75
4.5	Four-Ball wear test.....	75
4.6	Reciprocating wear test.....	76
4.6.1	General condition of the specimen after the test .....	76
4.6.2	Surface characterisation under high magnification.....	81
4.6.3	Overview on the surface profile of worn area.....	87
4.6.4	Surface roughness .....	91
4.6.5	Oil retention volume .....	94
4.6.6	Wear volume .....	97
4.6.7	Wear depth .....	102

4.6.8 Friction test .....	107
CHAPTER FIVE CONCLUSIONS AND RECOMMENDATIONS.....	111
5.1 Conclusion .....	111
5.2 Recommendation .....	112
REFERENCES.....	114
APPENDIX A Calculating the kinematic viscosity .....	122
APPENDIX B IFM data of the uncoated liner with SAE 40.....	123
APPENDIX C IFM data of the uncoated liner with SAE 5W-30.....	125
APPENDIX D IFM data of the coated liner with SAE 5W-30.....	127

## LIST OF TABLES

Table 3.1: Wear test simulator specification.....	38
Table 3.2: Chemical composition of the cast AlSi-alloy JIS - ADC12 .....	39
Table 3.3: Characteristics of employed lubricants (Petronas, 2011) .....	42
Table 3.4: Bath composition of zincate process.....	55
Table 3.5: Bath composition of electroless Ni-P-C <sub>g</sub> -SiC coating .....	57
Table 4.1: Maximum compression load versus compression displacement .....	64
Table 4.2: Piston ring specification.....	65
Table 4.3: Specimen Vickers hardness against temperature .....	75
Table 4.4: Result of four-ball wear test for SAE 40 and SAE 5W-30.....	76



## LIST OF FIGURES

Figure 1.1: Mechanical losses distribution in an internal combustion engine (Taylor, 1998) .....	1
Figure 2.1: Surface profile of a cylinder liner at TDC of an operated engine after 400,000 miles (Radil, 1996).....	6
Figure 2.2: a) Wear, b) wear rate, and c) surface roughness, as a function of engine break-in time (Ma, Henein, Bryzik, and Glidewell, 1998) .....	7
Figure 2.3: Diesel engine cylinder wall at top dead centre after long term running (Priest and Taylor, 2000).....	9
Figure 2.4: Wear estimation after matching 90% point of bearing area curve, a) before, and b) after the test (Kumar, Kumar, Prakash and Sethuramiah, 2000) .....	10
Figure 2.5: Average wear depth of cylinder bore and wear rate versus time (Gara et al., 2010).....	14
Figure 2.6: A maximum peak height $R_p$ and a maximum valley depth $R_v$ surface profile parameters and their interpretation on the material ratio (Mr) curve (Michalski and Woś, 2011) .....	15
Figure 2.7: Temperature distribution of cylinder bore in an IC engine (Rajput, 2005) .....	17
Figure 2.8: Stribeck curve according to Sommerfeld number (Bryant, 2005).....	19
Figure 2.9: Stribeck curve according to film thickness ratio, $\lambda$ (Gohar and Rahnejat, 2008) .....	20
Figure 2.10: The micro hardness of Ni-P and Ni-P composite coatings at as-deposited, 200, 300, 400 and 500°C for 1 hour heat treatment, respectively (Wu, Lei, Shen and Hu, 2006).....	28

Figure 3.1: Schematic of the test rig .....	34
Figure 3.2: Cross-section of the reciprocating wear tester.....	36
Figure 3.3: CAD illustration of the reciprocating wear tester set up .....	37
Figure 3.4: Actual set up of the reciprocating wear tester .....	37
Figure 3.5: Piston ring holder assembly, a) before, and b) after assembled .....	39
Figure 3.6: a) AlSi-alloy ADC12 ingot, b) Wire cut process, c) Liner specimen.....	39
Figure 3.7: Viscosity against temperature between 140°C and 180°C of lubricant type (Widman, 2009) .....	41
Figure 3.8: The marked position and evaluation area of the specimens, a) liner, and b) piston ring .....	42
Figure 3.9: Measurement of elastic tension of piston ring by UTM.....	43
Figure 3.10: a) Vickers hardness measurement at elevated temperature, and b) closed up on the piston ring specimen.....	44
Figure 3.11: Alicona Infinite Focus G4 Microscope .....	45
Figure 3.12: The $R_a$ parameter derivation (Smith, 2001).....	46
Figure 3.13: Bearing ratio changes with depth (ISO 13565-2, 1996).....	46
Figure 3.14: Bearing ratio curve (Alicona Imaging, 2007).....	47
Figure 3.15: Bearing ratio curve with its parameters (Gara et al., 2010).....	48
Figure 3.16: Wear depth measurement of a surface profile .....	51
Figure 3.17: Four Ball wear tester DUCOM TR-30L-IAS (Ducom, 2011) .....	51

Figure 3.18: Ball pot assembly (Ducom, 2011) .....	52
Figure 3.19: Image acquisition system to measure area of the wear scars (Ducom, 2011) .....	53
Figure 3.20: a) Set up for electroless coating system, and b) Closed up of the coating process.....	56
Figure 3.21: Heat treatment at 400°C for one hour.....	59
Figure 3.22: Flowchart for the overall methodology of the study .....	63
Figure 4.1: Free body diagram of the piston ring .....	65
Figure 4.2: a) Uncoated AlSi-alloy ADC12 liner specimen, and b) Coated liner specimen with electroless Ni-P-C <sub>g</sub> -SiC composite coating .....	66
Figure 4.3: Coating thickness in a single plating bath after; a) 1 hour, and b) 3 hours .....	66
Figure 4.4: FESEM cross-section image and film thickness of the Ni-P-C <sub>g</sub> -SiC composite coating on AlSi-alloy substrate under different magnifications, a) 50X, b) 500X, and c) 1000X. ....	68
Figure 4.5: EDX analysis on cross-sectional view of the composite coating .....	69
Figure 4.6: EDX analysis of the surface of the composite coating.....	70
Figure 4.7: FESEM surface micrograph of a) AlSi-alloy ADC12 substrate, b) as per coated electroless Ni-P-C <sub>g</sub> -SiC, c) Stress relieving (190°C/3 hr) electroless Ni-P-C <sub>g</sub> -SiC, and d) Heat treated (400°C/1 hr) electroless Ni-P-C <sub>g</sub> -SiC.....	71
Figure 4.8: XRD patterns of a) AlSi-alloy ADC12, b) as per deposited Ni-P-C <sub>g</sub> -SiC, c) annealed 190°C for 3 hours, and d) heat treated 400°C for 1 hour.....	73

Figure 4.9: Relationship between micro hardness and post-treatment procedures of electroless Ni-P-C <sub>g</sub> -SiC composite coating .....	74
Figure 4.10: Micro hardness of AlSi-alloy ADC12 substrate after post-treatment procedures .....	74
Figure 4.11: General condition of AlSi alloy liners after 100 hours reciprocating wear test; a) uncoated liner with SAE 40 lubrication, b) uncoated liner with SAE 5W-30 lubrication, c) Coated liner with SAE 5W-30 lubrication.....	77
Figure 4.12: The EDX of burnt SAE 40 lubricant .....	77
Figure 4.13: The EDX of burnt SAE 5W-30 lubricant of the coated specimen .....	78
Figure 4.14: The EDX of worn area of the coated specimen.....	78
Figure 4.15: Surface condition of AlSi-alloy liners before and after 100 hours reciprocating wear test under different test parameters .....	79
Figure 4.16: Surface condition of piston rings before and after reciprocating wear test under different test parameters.....	80
Figure 4.17: Cross section view (A-A) of original piston ring for coated liner with SAE 5W-30 lubricant after 20 hours.....	81
Figure 4.18: Evaluation area of uncoated AlSi-alloy liner under reciprocating wear test with SAE 40 lubricant .....	82
Figure 4.19: Micro pitting at DC1 area of uncoated liner with SAE 40 lubricant.....	83
Figure 4.20: Evaluation area of uncoated AlSi-alloy liner under reciprocating wear test with SAE 5W-30 lubricant .....	83
Figure 4.21: Evaluation area of coated AlSi-alloy liner under reciprocating wear test with SAE 5W-30 lubricant.....	84

Figure 4.22: Evaluation area of piston ring paired with uncoated AlSi-alloy liner under reciprocating wear test with SAE 40 lubricant .....	85
Figure 4.23: Evaluation area of piston ring paired with uncoated AlSi-alloy liner under reciprocating wear test with SAE 5W-30 lubricant .....	86
Figure 4.24: Evaluation area of piston ring paired with coated AlSi-alloy liner under reciprocating wear test with SAE 5W-30 lubricant .....	87
Figure 4.25: Worn surface profile of the liner specimens.....	89
Figure 4.26: Worn surface profile of the piston rings.....	90
Figure 4.27: $R_a$ vs. time for uncoated liner with SAE 40 lubricant .....	92
Figure 4.28: $R_a$ vs. time for uncoated liner with SAE 5W-30 lubricant .....	93
Figure 4.29: $R_a$ vs. time for coated liner with SAE 5W-30 lubricant .....	94
Figure 4.30: $V_o$ vs. time for uncoated liner with SAE 40 lubricant.....	95
Figure 4.31: $V_o$ vs. time for uncoated liner with SAE 5W-30 lubricant.....	96
Figure 4.32: $V_o$ vs. time for coated liner with SAE 5W-30 lubricant.....	96
Figure 4.33: Accumulative wear volume in scanned area $A_M$ vs. time, for uncoated liner with SAE 40 lubricant.....	98
Figure 4.34: Accumulative wear volume in scanned area $A_M$ vs. time, for uncoated liner with SAE 5W-30 lubricant .....	99
Figure 4.35: Accumulative wear volume in scanned area $A_M$ vs. time, for coated liner with SAE 5W-30 lubricant.....	100
Figure 4.36: Accumulative wear volume after 100 hours of the wear test .....	101

Figure 4.37: Wear depth and wear rate vs. time, for uncoated liner with SAE 40 lubricant.....	103
Figure 4.38: Wear depth and wear rate vs. time, for uncoated liner with SAE 5W-30 lubricant.....	104
Figure 4.39: Wear depth and wear rate vs. time, for coated liner with SAE 5W-30 lubricant.....	105
Figure 4.40: Wear depth after 100 hours of the wear test.....	107
Figure 4.41: Frictional modes of the liner specimens normalised to the position stroke after 100 hours of the test at 200°C.....	108
Figure 4.42: Friction coefficient of the liner specimens at DC1, DC2 and middle stroke after 100 hours of the test.....	110

## NOMENCLATURE

A	: Area [ $\mu\text{m}^2$ ]
$A_k$	: Area related to the core material [ $\mu\text{m}^2$ ]
$A_M$	: surface area measured by IFM [ $\mu\text{m}^2$ ]
$A_p$	: Area related to the peaks [ $\mu\text{m}^2$ ]
$A_s$	: Surface area of indentation [ $\text{mm}^2$ ]
$A_v$	: Area related to the valley material [ $\mu\text{m}^2$ ]
Al	: Aluminium
AlSi	: Aluminium silicon
ASTM	: American Society for Testing and Materials
a.u.	: Arbitrary unit
BDC	: Bottom dead centre
BN	: Boron nitride
BS	: British Standard
C	: Carbon
CA	: Castor oil
Ca	: Calcium
$\text{CH}_3\text{CH}_2\text{COOH}$	: Propionic acid
$\text{CH}_3\text{COONa}\cdot 3\text{H}_2\text{O}$	: Sodium acetate trihydrate
$\text{C}_{19}\text{H}_{42}\text{NBr}$	: Cetyltrimethylammonium (cetrimonium) bromide (CTAB)
$\text{C}_3\text{H}_6\text{O}_3$	: Lactic acid
$\text{C}_g$	: Graphite
$\text{CO}_2$	: Carbon Dioxide
Cr	: Chromium
CTAB	: Cetyltrimethylammonium (cetrimonium) bromide
Cu	: Copper

CuK $\alpha$	: X-ray diffraction energy from copper electrode
cSt	: Centistokes
d	: Mean diagonal of indentation [mm]
D	: Diameter
DC	: Dead centre
EDX	: Energy dispersive X-ray spectroscopy
EHD	: Elasto-hydrodynamic
EHL	: Elasto-hydrodynamic lubrication
EN	: Electroless nickel
F	: Force or tension [N]
Fe	: Iron
FeCl	: Ferric chloride
FESEM	: Field emission scanning electron microscope
h	: Height [ $\mu\text{m}$ ]
H <sub>2</sub> O	: Water
HCl	: Hydrochloric acid
HNO <sub>3</sub>	: Nitric acid
HV	: Vickers hardness
IC	: Internal combustion
ICSD	: Inorganic Crystal Structure Database
IFM	: Infinite Focus G4 Microscope
IMC	: Integrated Measurement & Control
ISO	: International Organization for Standardization
JIS	: Japanese industrial standards
KNaC <sub>4</sub> H <sub>4</sub> O <sub>6</sub> ·4H <sub>2</sub> O	: Potassium sodium tartrate
Mg	: Magnesium



MMC	: Metal Matrix Composite
Mn	: Manganese
MoS <sub>2</sub>	: Molybdenum Disulfide
Mr	: Material ratio
NaH <sub>2</sub> PO <sub>2</sub> •H <sub>2</sub> O	: Sodium hypophosphite hydrate
NaNO <sub>3</sub>	: Sodium nitrate
NaOH	: Sodium hydroxide
Ni	: Nickel
Ni-P	: Nickel-phosphorus
Ni <sub>3</sub> P	: Nickel phosphide
NiSO <sub>4</sub> •6H <sub>2</sub> O	: Nickel (II) sulphate hexahydrate
O	: Oxygen
P	: Phosphor
<i>P</i>	: Pressure [Pa]
<i>P<sub>L</sub></i>	: Load [kgf]
Pb	: Lead
Pb(NO <sub>3</sub> ) <sub>2</sub>	: Lead nitrate
POME	: Palm oil methyl ester
PTFE	: Polytetrafluoroethylene
PTWA	: Plasma Transferred Wire Arc
PVD	: Physical vapour deposition
R <sub>a</sub>	: Average roughness [μm]
R <sub>k</sub>	: Core roughness depth [μm]
R <sub>mr1</sub> or m <sub>r1</sub>	: Material ratio corresponding to the upper limit of the roughness core [%]
R <sub>mr2</sub> or m <sub>r2</sub>	: Material ratio corresponding to the lower limit of the roughness core [%]

$R_p$	: Material fraction of the surface layer [ $\mu\text{m}$ ]
$R_{pk}$	: Reduced peak height [ $\mu\text{m}$ ]
$R_q$	: Root mean square height [ $\mu\text{m}$ ]
$R_v$	: Material fraction of the oil retention volume [ $\mu\text{m}$ ]
$R_{vk}$	: Reduced valley depth [ $\mu\text{m}$ ]
RT	: Room temperature
S	: Sulphur
$So$	: Sommerfeld number [-]
SAE	: Society of Automotive Engineers
SBME	: Soya bean methyl ester
SBO	: Soya bean oil
SEM	: Scanning electron microscope
Si	: Silicon
SiC	: Silicon carbide
SRV	: Schwingungs-, Reibungs- und Verschleisstest (German language for vibration-, friction- and wear test)
T	: Thickness [mm]
TDC	: Top dead centre
Ti	: Titanium
TRR	: Top-ring reversal
UTM	: Universal testing machine
$V_o$	: Oil retention volume [ $\mu\text{m}^3/\mu\text{m}^2$ ]
$v$	: relative speed [ $\text{ms}^{-1}$ ]
V	: Volume [ $\mu\text{m}^3$ ]
$V_k$	: Volume related to the core material [ $\mu\text{m}^3$ ]
$V_p$	: Volume related to the peaks [ $\mu\text{m}^3$ ]

$V_{\text{total.after}}$	: Volume after the test [ $\mu\text{m}^3$ ]
$V_{\text{total.before}}$	: Volume before the test [ $\mu\text{m}^3$ ]
$V_v$	: Volume related to the valley material [ $\mu\text{m}^3$ ]
$W$	: Width [mm]
$W_{\text{depth}}$	: Wear depth [ $\mu\text{m}$ ]
$W_{\text{vol}}$	: Wear volume [ $10^3 \cdot \mu\text{m}^3$ ]
$W_{\text{rate}}$	: Wear rate [ $\mu\text{m}/\text{h}$ ]
wt. %	: Weight percentage [%]
XRD	: X-ray diffraction
Zn	: Zinc
ZnO	: Zinc oxide
$\alpha$	: Face angle of indenter [ $^\circ$ ]
$\lambda$	: Film thickness ratio [-]
$\mu$	: Friction coefficient
$\pi$	: Pi
$\eta$	: Dynamic viscosity [mPas]

# **KESAN SALUTAN TANPA ELEKTRO TERHADAP KEHAUSAN DAN GESERAN DI PERMUKAAN PELAPIK SILINDER AISI**

## **ABSTRAK**

Sebuah simulator ombok - pelapik dengan panjang lejang 15mm telah direkabentuk bagi membolehkan ujikaji dijalankan pada kelajuan maksimum 500rpm dengan suhu 300°C. Spesimen aluminium-silikon (AlSi) aloi disediakan dari aloi AlSi tuang (ADC12) dan dipotong bagi membentuk susuk bulat yang mewakili silinder bergaris pusat 36mm. Spesimen ini kemudiannya disalut melalui proses tanpa elektro dengan salutan komposit Ni-P-C<sub>g</sub>-SiC yang menghasilkan ketebalan nominal 35µm. Penyelidikan ini meliputi kajian tentang tahap kehausan dan pengukuran geseran pada 300rpm dan 200°C menggunakan minyak mineral SAE 40 dan minyak semi-sintetik SAE 5W-30.

Pengukuran haus dinilai secara progresif bagi 100 jam ujian haus menggunakan Mikroskop Alicona Infinite Fokus G4. Pemantauan yang dilakukan merangkumi kedalaman, kadar dan isipadu haus bersama-sama dengan kekasaran permukaan. Bagi pelapik tidak bersalut, purata kekasaran ( $R_a$ ) berkurang dengan masa memandangkan semasa eksperimen permukaan menjadi semakin licin disebabkan oleh kehilangan puncak-puncak permukaan sebelum mencapai keadaan mantap. Trend ini adalah selari dengan apa yang diperolehi oleh penyelidik-penyelidik sebelum ini. Trend isipadu dan kedalaman haus untuk pelapik tidak bersalut juga adalah amat serupa. Kadar haus yang lebih tinggi pada peringkat awal sebelum mencapai keadaan mantap adalah setara dengan kajian-kajian sebelum ini. Bagi pelapik bersalut pula, keunggulan ketahanan haus salutan komposit Ni-P-C<sub>g</sub>-SiC pada pelapik AlSi aloi, bertahan hanya sehingga 40 jam daripada ujian haus sahaja. Selepas 60 jam ujian, satu fenomena lesu pada subpermukaan yang

mengakibatkan pengelupasan di sebahagian filem salutan dapat diperhatikan. Secara umumnya, haus tertinggi berlaku di pusat-pusat mati berbanding di strok tengah, dengan kedalaman haus maksimum bagi pelapik bersalut adalah  $14.4\mu\text{m}$ , diikuti dengan  $6.4\mu\text{m}$  bagi pelapik tidak bersalut berpelincir SAE 40 dan  $6.3\mu\text{m}$  bagi pelapik tidak bersalut berpelincir SAE 5W-30. Bagi gelang omboh yang tahap kekerasannya lebih tinggi berbanding pelapik AlSi aloi yang tidak bersalut, kedalaman haus adalah minimum. Walaubagaimanapun, haus gelang omboh yang berpasangan dengan pelapik bersalut adalah sangat teruk dengan kedalaman haus berjumlah  $315\mu\text{m}$  direkodkan. Ini disebabkan oleh filem salutan komposit Ni-P-C<sub>g</sub>-SiC yang kasar dan lebih keras.

Pengukuran daya geseran menunjukkan bahawa perbezaan nilai pekali geseran ( $\mu$ ) di setiap lokasi, bagi spesimen pelapik bersalut dan tidak bersalut, dengan menggunakan minyak pelincir berbeza adalah sangat kecil. Nilai  $\mu$  tertinggi adalah dicatat pada pusat-pusat mati yang julatnya antara 0.18 hingga 0.19, manakala di strok tengah berkisar antara 0.10 dan 0.11. Malangnya, kesan zarah grafit sebagai pengurang geseran bagi pelapik bersalut tidak dapat diperhatikan dalam kajian ini. Malah, pelapik yang tidak bersalut menghasilkan nilai  $\mu$  yang lebih rendah.

# **EFFECT OF ELECTROLESS PLATING ON WEAR AND SURFACE FRICTION OF AISi CYLINDER LINER**

## **ABSTRACT**

A piston - liner wear simulator with a stroke length of 15mm is developed which can carry out testing at maximum speed of 500 rpm with temperature of 300°C. Aluminium-silicon (AlSi) alloy specimens are prepared from cast the AlSi alloy (ADC12) and cut to shape representing the circular profile of a 36mm diameter cylinder. The specimen is coated using electroless process with Ni-P-C<sub>g</sub>-SiC composite coating of 35µm nominal thickness. The study covers the wear and friction measurement at 300 rpm and 200°C using the mineral oil SAE 40 and semi-synthetic oil SAE 5W-30.

Wear measurement is evaluated progressively for 100 hours of the wear test using Alicona Infinite Focus G4 Microscope where the wear- depth, rate and volume together with the surface roughness are monitored. For the uncoated liners, the average roughness ( $R_a$ ) decreases with time as the surface became smoother because of the surface peaks being removed during the experiment before it reaches a steady state. This trend is comparable to what have been obtained by previous researchers. The trends of the wear volume and wear depth for the uncoated liners are also very similar. The higher wear rate in the beginning before reaching steady state is comparable to the previous studies. Meanwhile, for the coated liner, the superior wear resistance of the Ni-P-C<sub>g</sub>-SiC composite coating on the AlSi-alloy liner withstand only up to 40 hours of the wear test. Subsequently, a subsurface fatigue phenomenon is observed after 60 hours of the test which resulted in the exfoliation of some part of the coating film. In general, the highest wear loss is at dead centres compared to the middle stroke with the maximum wear depth for the coated liner is

14.4 $\mu\text{m}$ , followed by 6.4 $\mu\text{m}$  for the uncoated liner with SAE 40 lubrication and 6.3 $\mu\text{m}$  for the uncoated liner with SAE 5W-30 lubrication, respectively. For the piston ring which is harder than the uncoated AlSi-alloy liner, the wear depth is minimal. However, severe wear loss with a total wear depth of 315 $\mu\text{m}$  is observed for the piston ring of the coated liner due to rougher and harder Ni-P-C<sub>g</sub>-SiC composite coating film.

Measurement of the friction force shows that the differences between friction coefficient ( $\mu$ ) values at each location of the coated and uncoated liner specimens with different lubricant types are very small with the highest  $\mu$  values is at dead centres which ranges between 0.18 to 0.19, while ranges between 0.10 to 0.11 at middle strokes. Unfortunately, the effect of the graphite particles as friction reducer for the coated liner is not observed in this study. In fact, the uncoated liner produces a lower  $\mu$  value.

# CHAPTER ONE

## INTRODUCTION

### 1.1 Background

The piston assembly consists of piston, piston rings and cylinder bore, are essential machine elements in a reciprocating engine. It was reported that 45% of the total energy losses in an internal combustion (IC) engine occurred in piston assembly due to frictional losses as shown in figure 1.1 (Taylor, 1998). It is generally understood that the mechanical properties of the materials applied in the piston assembly, including their tribological characteristics, would directly influence the engine performance. Therefore, enhanced material performance for these applications have continuously been sought for better friction and wear performances.

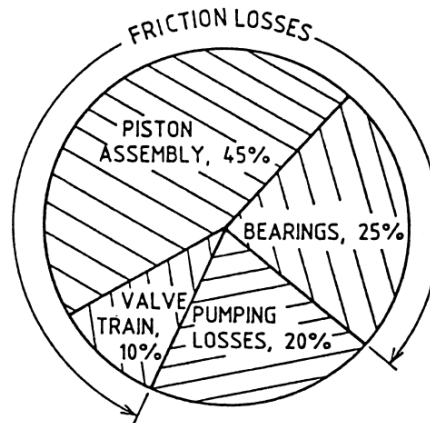


Figure 1.1: Mechanical losses distribution in an internal combustion engine (Taylor, 1998)

Nowadays, cast AlSi-alloys are increasingly being used in automotive engine cylinder blocks and liners as an alternative to the conventional cast iron. The main reason is that AlSi-alloys are lighter with better heat conductivity. The alloys are also widely used for mass production of components such as pistons, cylinder heads, and



wheels. Silicon particles in the compound enhance the mechanical properties of the alloy since the seizure of aluminium readily occur when subjected to sliding contact. However, compared to cast iron, AlSi-alloys have lower wear resistance. In view of the AlSi-alloy used as cylinder block material, it will suffer from material loss when subjected to sliding contact against the piston ring. Therefore variant of coatings have been applied to overcome this setback.

## **1.2 Problem statement**

Cast AlSi-alloys are widely used in the automotive industries as the cylinder block material because of its light weight. Moreover, the use of sleeveless cast AlSi-alloy cylinder block with much lower wear resistance compared to cast iron forces the automotive manufacturer to protect the inner face of the cylinder bore from wear with durable layer of coating. Many researchers have studied the potential plating materials and their effect on the friction coefficient and wear resistance. It is reported that the electroless nickel - phosphor - graphite - silicon carbide (Ni-P-C<sub>g</sub>-SiC) composite coating has the advantage of low friction coefficient and high wear resistance due to incorporated C<sub>g</sub> and SiC particles in the coating film, respectively (Wu, Lei, Shen and Hu 2006). However, the effect of this coating on tribological performance of the AlSi-alloy cylinder liner and piston ring interface is yet to be discovered. On the other hand, there are numerous technical difficulties in the evaluation of the tribological performance of the piston assembly in an actual IC engine and many researchers are using reciprocating tribological tester to study and understand the wear and friction mechanism. It is well-known that the severe wear on the cylinder bore/liner inner face occurs at the top dead centre (TDC) because of high pressure, starved lubrication and high temperature where it is reported to be

around 200°C (Radil, 1996 and Rajput, 2005). However, in many reported laboratory experiments, the test temperature is much lower than the actual maximum temperature at TDC. Furthermore, different lubricant will have different tribological characteristics. Therefore, there is a need to identify the relationship between surface roughness, wear and friction behaviour of the cylinder liner and piston ring interface at the elevated temperature of the IC engine with different type of lubricants.

### **1.3 Research objective**

The hypothesis of this study is the surface roughness of the AlSi-alloy liner, and the lubricant types will influence the tribological performance of the cylinder liner and piston ring interface. Meanwhile, the protective coating layer on the AlSi-alloy liner is to enhance its wear resistance and reduce the friction. The objectives of this research are:

- To assess the effect of different lubricants on the tribological characteristics of the AlSi-alloy cylinder liner and piston ring interface using the reciprocating wear tester.
- To evaluate the effect of electroless Ni-P-C<sub>g</sub>-SiC composite coating on the wear and friction properties of coated AlSi-alloy liner against piston ring using the reciprocating wear tester.

### **1.4 Scope of research**

The scope of the study is mainly about determining wear and friction of the AlSi-alloy cylinder liner and piston ring under reciprocating wear test. The surface roughness parameters are also measured in order to understand the wear and friction mechanism. The tribological performance of the electroless Ni-P-C<sub>g</sub>-SiC coated

AlSi-alloy liner is compared with the uncoated liner. The test is conducted with two different commercial engine lubricants. The data are measured periodically up to 100 hours of test duration.

## **1.5 Thesis outline**

The thesis is presented in five chapters including introduction, literature review, methodology, results and discussion and finally conclusion. Chapter One consists of background of the study, research objectives and thesis outline. Chapter Two consists of the literature review. The previous work done by other researchers regarding to the tribological analysis of piston ring-cylinder liner interface, and also electroless nickel coating are reviewed and discussed. Chapter Three describes the methodology used in this study including fabrication of the reciprocating test rig. Chapter Four presents the results and also the discussion on the outcomes. Chapter Five presents the conclusion and recommendation of the present work.

## **CHAPTER TWO**

### **LITERATURE REVIEW**

#### **2.1 Overview**

This chapter reviews the work related to wear and friction study of piston assembly, basic lubrication regimes, lubrication performances and electroless nickel composite coating.

#### **2.2 Tribological performance study of piston assembly**

Published data on wear and friction of cylinder liner and piston ring of the IC engine are very limited because of the technical difficulties to carry out the measurement inside the cylinder bore. Several experimental methods and bench tests have been made to simplify and simulate the wear and friction between cylinder wall and piston ring as close as possible to the IC engine condition. Tribological testers such as pin-on-disc testers, block-on-ring testers and etc. have been widely employed as preliminary tribological study of the piston assembly (Takami et al., 2000; Jensen, Bøttiger, Reitz and Benzion, 2002; and Srivastava, Agarwal and Kumar, 2007).

Surface topography features at different longitudinal positions of cylinder liners were investigated by Dong, Davis, Butler and Stout (1995). By using a comprehensive three-dimensional characterisation technique, different locations of the liner displayed different topographic features and different functional properties. The results showed that wear of the cylinder liner along the longitudinal axis was uneven. Generally, wear of the cylinder liner mostly took place at peak and core zones of the surface topography, whereas valley zone was less affected. Severe wear has also been observed at top dead centre (TDC) and bottom dead centre (BDC) area compared to the middle area of the stroke.

In 1996, Radil developed a tribological test method to measure wear and friction between candidate piston ring and cylinder liner coatings for advance heavy duty diesel engines. A reciprocating test rig was employed to replicate the boundary lubricated condition as in the top-ring reversal (TRR) point of piston ring and cylinder liner interface, where piston ring is at TDC. Commercially chrome coated piston rings and pearlitic gray cast iron cylinder liners were utilised for this experiment. The test was conducted with 15mm stroke at constant speed of 20Hz, static load of 192N and at temperature of 200°C for 24 hours. Engine oil SAE 15W-40 was dropped every 20 seconds for lubrication purpose. The friction coefficient obtained from the test ranging from 0.079 to 0.082 and the mean wear factors of the ring and liner were  $7.28 \times 10^{-10}$  and  $2.62 \times 10^{-8}$  mm<sup>3</sup>/Nm, respectively. While the wear factors for ring and liner calculated from an actual operated engine was  $4.44 \times 10^{-10}$  and  $1.60 \times 10^{-9}$  mm<sup>3</sup>/Nm, respectively. The inspection on the surface profile of the actual operated engine confirmed that the maximum wear occurred at TDC with maximum wear depth of 0.05 mm as shown in figure 2.1. Radil also concluded that the test method was capable to mimic the TRR condition of the actual operated engine.

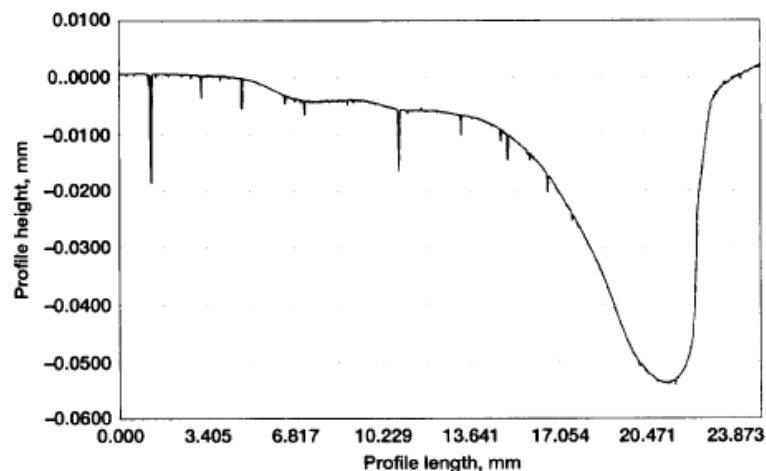


Figure 2.1: Surface profile of a cylinder liner at TDC of an operated engine after 400,000 miles (Radil, 1996)

Ma, Henein, Bryzik, and Glidewell (1998) measured time-dependant wear and surface roughness of cylinder liner at the TDC area of a single cylinder, air cooled gasoline engine during break-in period. The test was conducted for 28 hours. Wear was measured by using a small wear probe that precisely fit into a hole in the cylinder liner at TDC area, and form a continuous surface with the liner surface. The advantage of this technique is that the wear probe can be removed without dismantling the engine. The highest surface roughness, friction and wear of the liner were observed at the beginning of the break-in period. The wear rate of the liner which is inversely proportional to the wear value dropped sharply at the beginning of the test, before it maintained a steady lower rate as shown in figure 2.2a and b. Figure 2.2c shows the surface roughness which steadily decreased over time and took longer than the wear rate to stabilise. The results concluded that friction was a linear function of the surface roughness and it was not an indicator for the wear rate.

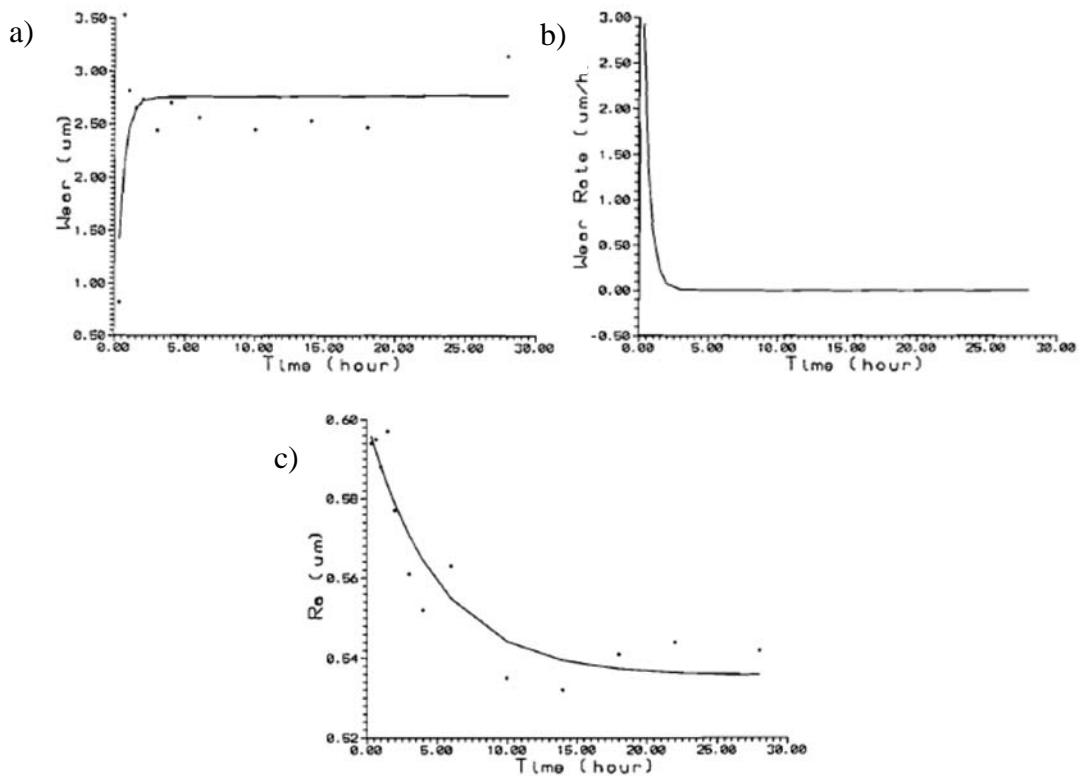


Figure 2.2: a) Wear, b) wear rate, and c) surface roughness, as a function of engine break-in time (Ma, Henein, Bryzik, and Glidewell, 1998)

Becker and Ludema (1999) investigated the important variables that influencing wear in a cylinder bore. A Cameron–Plint high frequency friction tester was used to accomplish the simulation with the stroke of 9 mm and the reciprocating frequency of 20 Hz. The temperature was varied from room temperature to 150°C and the load ranged from 30 to 240 N. Wear results from the simulator showed similar characteristics to the engines. The relative importance of the influential wear variables such as lubricant contributions, material properties, load and temperature could be determined by the model simulator. In the study, the ring material showed a strong effect on the wear result of cylinder bore.

Priest, Dowson and Taylor (1999) developed a novel interactive numerical model to predict the dynamics, lubrication and wear of piston rings under fired condition of a diesel engine. The model was applied to study the effect of lubrication performance on tribological characteristics of measured ring packs before and after running periods. It was also used to calculate the lubrication and wear performance of the top compression ring. During the engine test, the surface roughness of the piston rings and the cylinder wall dramatically reduced over the test period. Their numerical method results had good correlation with the experimental result of the measured top compression ring profiles.

The surface profile and topography of cylinder wall of the gasoline and diesel engine were studied by Priest and Taylor (2000) where the cylinder walls were manufactured from grey cast iron. The least wear of the cylinder wall was observed at middle stroke region. Furthermore, after running more than 628 hours of the diesel engine, the cylinder wall profile at the upstroke region was clearly marked with the location of the ring reversal points as shown in figure 2.3, where the maximum wear depth was observed at the reversal point of ring 1 compared to the other rings. This

happened due to the low film thicknesses and high loads of the combustion pressure at these points.

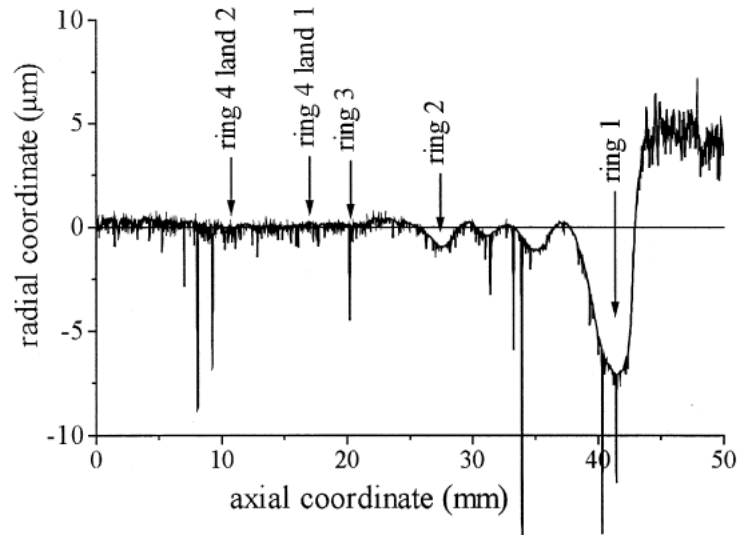


Figure 2.3: Diesel engine cylinder wall at top dead centre after long term running (Priest and Taylor, 2000)

A unique procedure to evaluate the wear volume and depth of the engine liner was proposed by Kumar, Kumar, Prakash and Sethuramiah (2000). However, this evaluation method is only valid as long as the valley depth is not totally removed during the wear process. This method suggested that after the wear test, the bearing area curve remains unchanged at 90% point as shown in figure 2.4. In this figure, the radial wear depth is the distance from point A to B which is obtained by the projection of the 70% to 30% line on the depth axis of the two bearing length curves. Then, the area between the overlapped bearing area curves, before and after the test was determined by numerical procedure. As the diameter of the liner is known, the wear volume at selected positions on the cylinder liner could be calculated. A special C++ programming was developed to assist the calculation. After 75 min of running, no clear wear trend is detected at TDC, middle stroke and BDC. By using usual



gauging procedure, the radial wear depth obtained ranging from 3 to 5 $\mu\text{m}$ , which is higher than this new procedure with the wear depth ranged from 0.25 to 1.9 $\mu\text{m}$ .

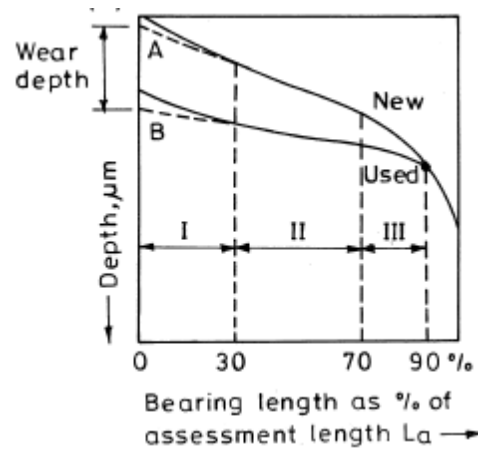


Figure 2.4: Wear estimation after matching 90% point of bearing area curve, a) before, and b) after the test (Kumar, Kumar, Prakash and Sethuramiah, 2000)

In 2000, Takami et al. of Toyota Central Research and Development Labs used a block-on-ring tester to perform a comparative evaluation of wear depth for different ring and bore materials before establishing correlation with on-engine testing. The sliding speed was set at 0.3m/s with a load of 1800 N for 30 minutes. However, the experimental set up of this tester is not representing the actual speed at the reversal point which is zero. The engine oil (SAE 5W-30) was used as lubricant for the test and gas nitrided ring was mated against various Metal Matrix Composite (MMC) materials. MMC material was used to reinforce the cylinder bore of the all aluminium alloy (JIS ADC12) cylinder blocks by using a laminar flow die cast process. From several MMC materials, 12 $\mu\text{m}$  mullite was favoured for the MMC bore material because of high tensile strength which resulted in 10 $\mu\text{m}$  and 3 $\mu\text{m}$  wear depth for the ring and bore respectively. The result showed that the wear of cylinder bore and ring material were well balanced when the MMC was reinforced by

crystallized alumina-silica fibre with the volume of mullite particle of 5% or higher. This was then verified by the actual engine durability test.

By using a simple pin-on-disc tester, Jensen, Bøttiger, Reitz and Benzon (2002) successfully conducted the wear simulation of the piston rings and cylinder liner interface for a two stroke marine diesel engine. The understanding of the wear phenomena such as smearing and scuffing was studied for the material selection. The new and existing materials were compared in terms of their tribological performance before a realistic test would be conducted. The evaluation of this method however is not based on the quantitative measurement rather it was based on the relative measurement. The mechanism of smoothing was detected after the test and it is noted that scuffing occur only when the surfaces are smooth. Hardness measurements showed that the virgin material is harder than the worn material.

An abrasive wear model for piston ring and cylinder bore interface by considering the effect of load, temperature, material properties, surface roughness and oil degradation during the steady state operation was developed by Tung and Huang (2004). This model which was developed based on a Cameron Plint simulator can be used either in theoretical modeling or integrated with finite element analysis. Based on this model simulation, the increases in the wear rate after a longer time are attributed to the high oil degradation rate used in this simulation. The lubricant oxidation and the surface delamination factor should also be concluded into the modeling in order to fully model the wear progression of piston ring/ cylinder bore system.

Pandazaras and Petropoulos (2004) proposed a method to monitor the wear of IC engine cylinder based on surface anisotropy which determines its lifetime. The experimental data was obtained by using a Renault friction-wear simulator with bore

diameter of 88 mm and piston stroke of 90 mm based on Renault 851 engine. Engine oil 15W-40 was used as lubricant and the test temperature was set at 120°C. Cast iron cylinder and rings were utilised as the tribo-elements. After a long operating time, the characteristic that exhibits the most variation of the cylinder surface parameters is the cylinder surface anisotropy. Surface anisotropy on the cylinder will produce a negative effect on the partial hydrodynamic lubrication and friction of the rings. From the experiment, the maximum wear and the cylinder surface anisotropy are interdependent. Since cylinder anisotropy has greater variability and sensitivity compared to other parameters, it should be considered as a cylinder wear criterion.

Srivastava, Agarwal and Kumar (2007) argued that several wear testers such as Cameron-Plint, SRV and Pin-on-disc tester does not reflect the true behaviour of an engine because of limitation of stroke length. A custom made non-firing engine simulator with stroke length of 82mm was used to measure wear behaviour of a production grade cylinder liner. The test was conducted at 1500 rpm at a constant load of 60N for 30 hours at room temperature. It was found that coefficient of friction in the system increases with the liner surface roughness. Towards the end of the experiment, the hard chrome plating of the ring worn out and the base material was exposed. The experiment also revealed that the maximum wear take place at TDC, whilst wear at BDC was higher than at mid-stroke location.

Tomanik (2008) investigated wear and friction behaviour of six different bore finishes including slide bore honing and structured laser bore against a PVD coated ring in the CERT UMT-2 reciprocating tester. The surface roughness parameter  $R_q$  (root mean square height) of these bore finishes ranged from 0.18 to 0.93 $\mu\text{m}$ . Each bore finish was tested with 50 and 100N load at six speed variant, and at ambient temperature. After four hours of the wear test, friction coefficient was reduced due to

break-in. Most of the finishes showed the boundary friction coefficient ( $\mu$ ) about 0.11 when lubricant condition approached the boundary regime. On the whole, the smoother surfaces resulted in lower ring and bore wear.

Lozano et al. (2009) evaluated the wear performance of the hypereutectic Al-Si-Cu alloy from an engine block by using a pin-on-disc tribometer. The test was conducted according to ASTM G99 standard with variable loads of 10, 30, 50, 120N, sliding speeds of 0.5, 1.0, 1.5m/s and sliding distances of 5, 10, 20km, under lubricated and unlubricated conditions. A steel ball was used as the pin element and engine oil SAE 40 was utilised as the lubricant. The result showed that the finer silicon particles distributed in the Al matrix provided the wear resistance to the alloy. It was observed that with higher loads and longer sliding distances, the friction coefficient would tend to diminish. Meanwhile, abrasive wear mechanism was observed in the unlubricated condition.

The effect of surface topography on friction and wear of cast iron cylinder liner was studied by Keller, Kapsa, Fridrici and Huard (2010) using a Cameron Plint TE77 test rig with a steel ball as the mate material. The test was performed with a normal load of 200N, the sliding frequency of 5Hz, the reciprocating stroke of 11mm and the temperature of 150°C. Engine oil SAE 5W-30 was used as the lubricant. It was concluded that the surfaces with higher surface asperities would delay the formation of protective tribochemical film, thus exhibited the highest wear. Different type of surfaces produced the different wear rate due to the difference in the protective tribofilm formation. As for the friction coefficient, a similar trend was observed for all type of surfaces, in which an increasing trend in the beginning stage of the test before decreasing and reaching a stable and constant value.

By using a repeatable replication process, Gara et al. (2010) measured the surface roughness and wear of the cylinder liner of a single cylinder diesel engine operated under a steady-state condition. The replicating material made from silicon rubber which is a liquid before curing could replicate the surface details with a resolution down to  $0.1\mu\text{m}$ . After cured, the replica was peeled away from the cylinder liner and measured by using the WYKO NT1 100 optical surface profilometer. The surface profiles were measured at the same spot before and after the test and the data were collected at 16 locations. By employing the bearing ratio parameters, a novel wear volume calculation method has been proposed which resulted in reasonable results compared with the wear results presented by other researchers. Results also showed that the decreasing rate of surface roughness with time is higher during the run-in period before it reached a steady state, as obtained by other researchers. The average wear depth and wear rate of the cylinder bore with time are plotted in figure 2.5. In this figure the wear rate is higher in the earlier stage and decreases with time, whereas for the wear depth it is vice versa. The average wear depth obtained in these results is much lower than Radil's results (1996).

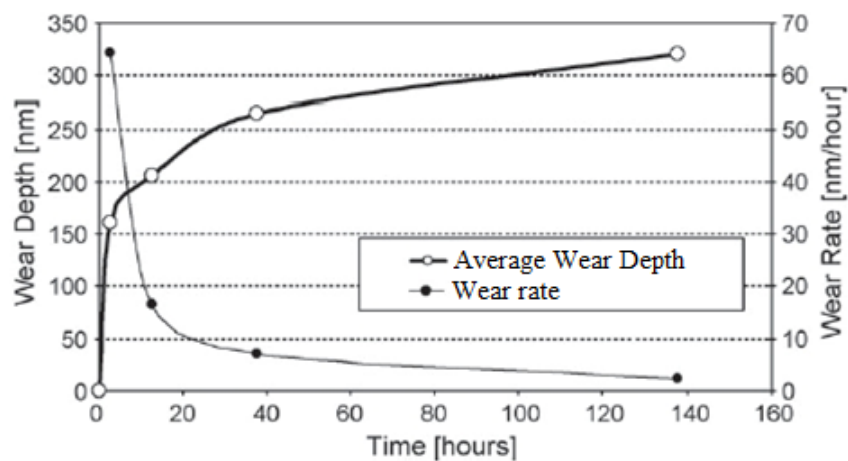


Figure 2.5: Average wear depth of cylinder bore and wear rate versus time (Gara et al., 2010)

The effect of the cylinder liner roughness parameters on the wear between piston-cylinder assembly of an air-cooled aircraft engine was investigated by Michalski and Woś (2011). To expedite the wear process, grinding flour was precisely dosed into the engine inlet manifold. Wear characteristics of piston-cylinder assembly with semi-synthetic oil 15W-50 lubrication were correlated with the parameters of the material ratio curve of the cylinder liner as shown in figure 2.6. In this figure the material ratio curve section is simplified to two separate parameters where  $R_p$  corresponds to the material fraction of the surface layer, and  $R_v$  to the oil retention volume. The result showed that the wear of all piston-cylinder parts decreased due to the lower value of the maximum valley depth  $R_v$  of the cylinder liner. Meanwhile, the higher value of maximum peak height  $R_p$  reduces the wear of the piston rings, but increases the wear of liner and piston.

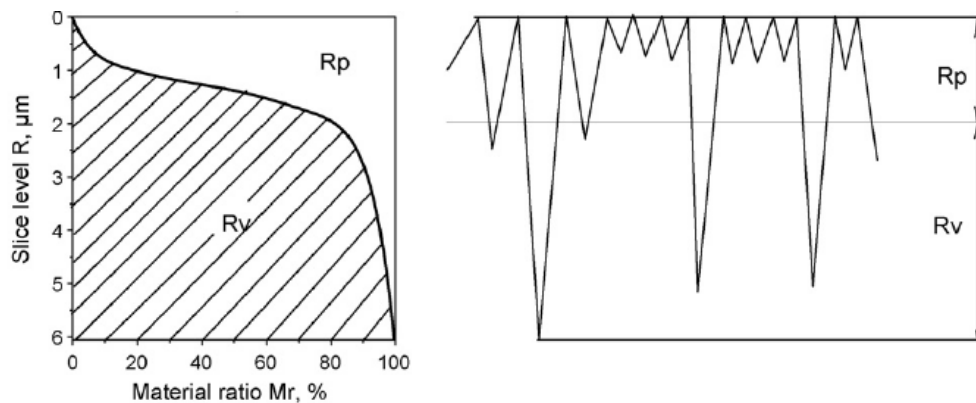


Figure 2.6: A maximum peak height  $R_p$  and a maximum valley depth  $R_v$  surface profile parameters and their interpretation on the material ratio (Mr) curve (Michalski and Woś, 2011)

An experimental study of friction and wear characteristics of piston ring and cylinder liner pair was performed by Kapsiz, Durat and Fecici (2011) by using Taguchi method. The reciprocating wear test was conducted according to ASTM G133-05 standard under lubricated condition with load varied from 60 to 80N,

speed of 50 to 150 rpm, temperature of 20°C, stroke of 100 mm for a distance of 2km. Commercial engine oil of SAE 10W-40 and 15W-40 were used as lubricant with feeding rate of 0.5ml/hour. Chrome coated piston ring and cast iron cylinder liner were used as the test specimens. The results showed that the friction coefficient was influenced mostly by the sliding velocity (68.14%), the oil type (14.15%) and the applied load (6.54%). The piston ring wear was influenced mostly by the sliding velocity (48.38%), the oil type (25.75%), and the applied load (12.10%). The cylinder liner wear was influenced mostly by the sliding velocity (44.60%), the applied load (41.54%), and the oil type (10.04%). In general, SAE 10W-40 lubricant gave better wear and friction characteristics to the piston ring and cylinder liner pair compared to SAE 15W-40 lubricant.

Recently, Sabeur, Ibrahim, Mohamed and Hassan (2012) optimized the cylinder liner finish based on experiment and a numerical prediction of elasto-hydrodynamic (EHL) friction in order to reduce the friction of cylinder ring-pack system. In the experiment, four cylinder liners made of gray cast iron were honed by using a vertical honing machine with an expansible tool (NAGEL 28-8470). With different honing process variables, the surface roughness parameters  $R_{pk}$  (reduced peak height) ranged from 0.217 to 1.308 $\mu\text{m}$ ,  $R_k$  (core roughness depth) from 0.510 to 3.403 $\mu\text{m}$  and  $R_{vk}$  (reduced valley depth) from 0.530 to 4.276 $\mu\text{m}$ . By utilizing a numerical model, the friction performance of the cylinder ring-pack system in an EHL regime was predicted based on the scanned three-dimensional surface topography of honed cylinder surfaces. The results showed that the hydrodynamic friction would increase as the increasing of the cylinder liner surface roughness with deeper valleys. The optimal hydrodynamic friction were obtained from the surface parameters of  $R_{pk} < 1\mu\text{m}$ ,  $R_k < 3\mu\text{m}$  and  $R_{vk} < 2.5\mu\text{m}$ , which resulted in  $\mu < 0.025$ .

### 2.3 Maximum temperature at TDC of an IC engine

Figure 2.7 shows the typical temperature distribution of a cylinder bore wall in a reciprocating IC engine related to the reversal positions of the piston. In this figure the temperature at TDC area of the first compression ring range between  $180^{\circ}\text{C}$  to  $230^{\circ}\text{C}$ , while at the BDC it is only around  $100^{\circ}\text{C}$  (Rajput, 2005).

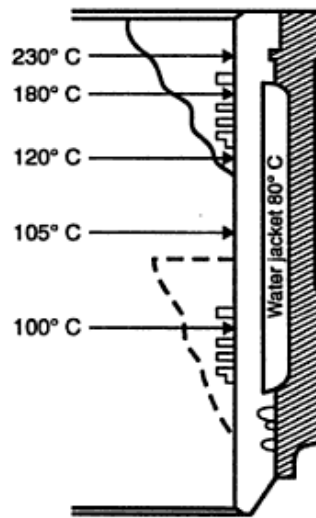


Figure 2.7: Temperature distribution of cylinder bore in an IC engine (Rajput, 2005)

To avoid burning of lubricant, Pischinger (2002) stated that the cooling feature of the piston assembly in an IC engine should be designed so that the maximum temperature of the lubricant must not exceed  $240^{\circ}\text{C}$ , which is the flash point for most of the engine oil. This requirement must also be considered during the piston and the cylinder bore design. This statement is in agreement with Toyama et al. (1983), where they emphasized that the temperature at TDC in an IC engine should be kept around  $200^{\circ}\text{C}$  in order to avoid scuffing of the ring and the cylinder bore wall by circulating the coolant through the cylinder head.



## 2.4 Lubrication

### 2.4.1 Lubrication regime and Stribeck curve

Lubricant is an important substance to preserve the longevity and reliability of the engine components. It has been introduced to reduce friction between moving parts within the engine, protecting them against wear, dissipating heat from the internal parts, carrying away contaminants or debris, preventing internal parts from corrosion and also improving the efficiency of the engine.

Lubrication state can be separated into three lubrication regimes corresponding to the thickness of the fluid film between the sliding surfaces. The ideal state of lubrication is called hydrodynamic lubrication where the sliding surfaces are fully separated by a fluid film. The boundary lubrication state occurs when the asperities of the two sliding surfaces are in contact and the effectiveness of the oil film is mostly lost. Mixed lubrication occurs where there are a mixture of the hydrodynamic and boundary lubrication between two sliding surfaces, in which the surfaces are partly in contact and partly separated (Hori, 2006). In addition, by including the elastic deformation of the contact faces and the influence of pressure on viscosity, the calculation on hydrodynamic lubrication films can be extended to elasto-hydrodynamic lubrication where two sliding surfaces are separated by a very thin fluid film (Mang and Dresel, 2007).

The friction or the lubrication condition is related to the viscosity, speed and load are graphically illustrated by the Stribeck curve as shown in figure 2.8. In this figure, the vertical axis represents the friction coefficient while the horizontal axis represents the Sommerfeld number ( $S_o = \eta \cdot v / P$ ), where  $\eta$  is the dynamic viscosity of the lubricant,  $v$  is the relative speed of the sliding surfaces and  $P$  is the pressure on

the interface. As the Sommerfeld number increases which indicates either increasing in speed or increasing in dynamic viscosity or reducing in pressure, the lubrication regime changes from boundary lubrication to mixed or elasto-hydrodynamic lubrication and finally to hydrodynamic lubrication. The zero point of Sommerfeld number indicates the static friction (Takadoun 2008).

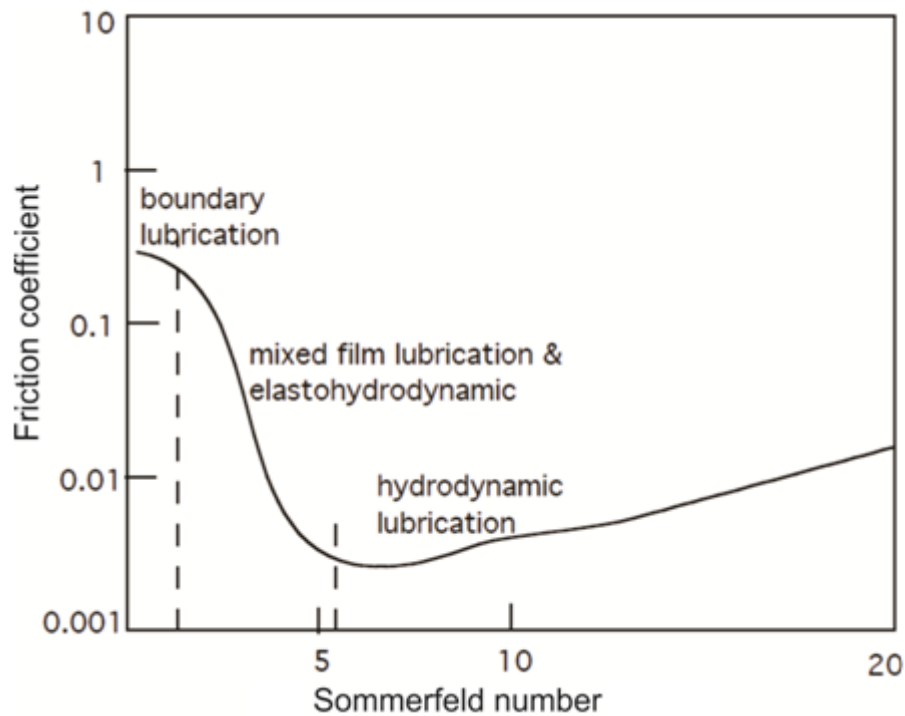


Figure 2.8: Stribeck curve according to Sommerfeld number (Bryant, 2005)

Later on the lubrication regimes are defined by the film thickness ratio ( $\lambda$ ) parameter, which is the ratio of the effective film thickness to the surface roughness as shown in figure 2.9 (Gohar and Rahnejat, 2008). In this figure, the Stribeck curve is devised, where the coefficient of friction is plotted against  $\lambda$  to determine the representative lubrication regimes. It is noted that the elasto-hydrodynamic and hydrodynamic lubrication occur only when  $\lambda$  value is bigger than three.

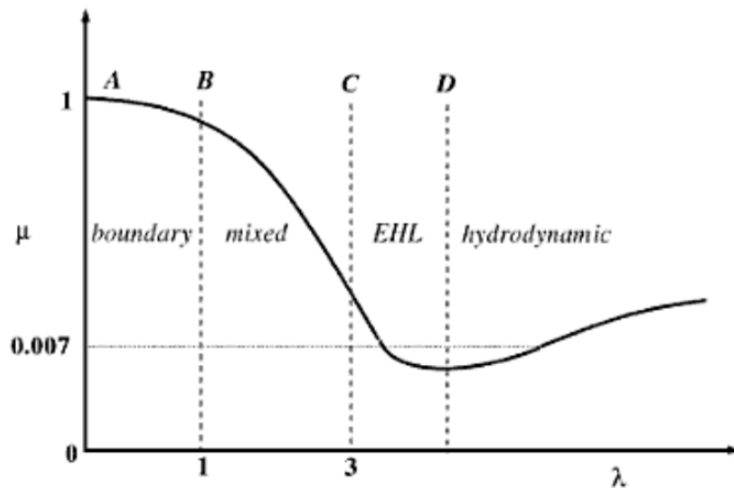


Figure 2.9: Stribeck curve according to film thickness ratio,  $\lambda$  (Gohar and Rahnejat, 2008)

#### 2.4.2 Lubrication performance studies

Masjuki, Maleque, Kubo and Nonaka (1999) compared the friction, wear, viscosity, oil degradation and exhaust emissions between palm oil and mineral oil-based lubricant. The test was carried out by using a universal reciprocating wear tester followed by in actual two-stroke engine test. The reciprocating wear test was conducted with pressure of 3.0 MPa, sliding speed of  $0.20\text{ms}^{-1}$ , temperature of  $25^\circ\text{C}$  and stroke of 80 mm. While in the actual engine test, the speed was set at 2800 rpm with various load applied for exhaust emission test but constant load was used for the wear test. The result showed that the palm oil which possess higher viscosity index and oxidation level, demonstrated better wear performance and more effective in carbon monoxide and hydrocarbon reduction in the exhaust emission. While the mineral based-oil showed better friction performance.

Truhan, Qu and Blau (2005) used a Cameron Plint test rig to evaluate the wear and friction of piston ring and cylinder liner materials in realistic engine oils for heavy duty diesel engine. The test was conducted with 10mm stroke at 600rpm with load from 20N to 240N at temperature range from  $20^\circ\text{C}$  to  $100^\circ\text{C}$ . Lubricants

including Jet-A aviation fuel, mineral oil, and a fully formulated 15W-40 heavy duty oil were used in the experiment. Generally, the friction coefficient increased very little with either load or temperature over the temperature range of 60–100°C where the fully formulated 15W-40 lubricant showed stronger temperature dependence. It was concluded that, all lubricants showed boundary lubrication behaviour at 100°C and the result shows that the relative wear rate of the liner compared to the ring was much higher than encountered in the actual engine.

The widespread use of coconut oil as two-stroke engine lubricant by auto rickshaw drivers in southern states of India made Jayadas, Prabhakaran Nair and Ajithkumar (2007) to scientifically evaluate its tribological performance. The experiment was carried out by using a four-ball tester, a test rig consisting of a two-stroke air cooled petrol engine and followed by on the road test. A commercial lubricant SAE 20W-50 was used for comparison purpose. In general, unmodified coconut oil has lower coefficient of friction and a good boundary lubricant but exhibits higher wear rate compared to SAE 20W-50 lubricant. The addition of 2% (by weight) of Zinc-Dialkyl-Dithio-Phosphate as an anti-wear/extreme pressure additive produced a significant improvement to the tribological behaviour of coconut oil.

Recently, Balamurugan, Kanagasabapathy and Mayilsamy (2010) conducted a study on soya bean oil (SBO) based lubricant for diesel engines. Various SBO formulations with biodegradable additives were tested for lubrication, wear, corrosion, thermal and oxidation properties, and compared with commercial engine oil SAE 40. The results demonstrated that the physico-chemical properties of SBOs are similar to the commercial mineral oil, whereas no significant difference were detected in engine performance and lube oil temperature compared to the commercial

lubricant. The soya bean methyl ester (SBME) blended with castor oil (CA), palm oil methyl ester (POME) and SAE 40 was found to be fit for crankcase applications, where POME and CA improved oxidation stability and wear resistance of the formulation.

## **2.5 Coating on AlSi -alloy cylinder bore**

A recent trend of an integral cast aluminium alloy-(Al-Si-Cu) engine block without a cast iron liner has been widely adopted in an IC engine development for optimum weight reduction (Enomoto and Yamamoto, 1998). The silicon particles in the aluminium alloy provide good wear resistance. Copper is also added to improve strength, hardness, thermal conductivity and form a basis of heat treatable aluminium alloy (Renshaw, 2004).

Wear resistance coatings on the inner face of a sleeveless cylinder were also developed in order to further improve their tribological characteristics. In 1967, the composite coating of nickel (Ni) and silicon carbide (SiC) has been introduced by the German company, Mahle to eliminate wear on aluminium-alloy cylinder bore with the trademark name of Nikasil. Soon, this coating is used by BMW, Porsche, Ferrari, Jaguar, Honda, Formula one car, NASCAR and motorcycle engines (Carley, 2008). However fuel quality issue in the 1980s which contained high level of sulphur lead to the failure of Nikasil-coated engine. Nowadays, it is reported that the low level of sulphur contain in the fuel is not sufficient to cause any problems to these coatings (Carley, 2008). Later, plasma sprayed coatings are growing in popularity in the automotive industry today which can be found in series of Volkswagen engines (Barbezat, 2005).

In 2008, Hariharan, Rajendran, Ganesh and Elansezhian examined the tribological performance of the electroless nickel (EN) coating on aluminium-alloy cylinder liner. Wear and friction test were carried out using pin-on-disc tribological tester with the sliding speed of 0.5m/s, sliding distance of 1000m and load of 30N at ambient temperature of 25°C. The average surface roughness ( $R_a$ ) of the aluminium alloy before and after coating are 1.70  $\mu\text{m}$  and 0.65  $\mu\text{m}$ , respectively. While the hardness measured is between 80-90Hv before coating and increased up to 500Hv after EN coating. The wear analysis showed that EN coated aluminium has lower wear rate and friction coefficient compared to the cast iron.

In order to reduce the friction and to form a novel wear resistant coating for the AlSi-alloy cylinder liners, Bobzin et al. (2008) used a special iron based materials called SUNA, for the Plasma Transferred Wire Arc (PTWA) internal diameter coating process. It is reported that by using thermal spray process, the same iron based wire feedstocks resulted in the coating with embedded boridic nanoscale precipitations. Cylinder bore walls of an in-line 4 cylinder engine made of aluminium EN AW 6060 are used as the coating substrates. The bond strength of the coating is measured nearly twice from the required value of 30MPa. However, the tribological characteristics of the coating are still under evaluation.

By using a focused  $\text{CO}_2$  laser beam and sintering of nanodiamond powders, Blum and Molian (2009) produced 50-75 $\mu\text{m}$  thick composite coating on cast aluminium-alloy A319. The tribological properties of the coating were evaluated by using ball-on-disc tester with static load of 5N, track radius of 2.5mm and speed of 50rpm for duration of 5 minutes. The ball made of stainless steel 440C was used as mate material. In spite of having a finer surface roughness ( $R_a = 1.8\mu\text{m}$ ), the uncoated specimen showed higher friction coefficient ( $\mu$  up to 1.03) compared to the

coated specimen with the  $R_a$  value of  $4.8\mu\text{m}$  which exhibited an average value of friction coefficient of 0.39. The result showed that the wear loss of the coated specimen is 5x less than the uncoated specimen. However, the wear on the stainless steel ball was not reported.

The effect of post treatment on the abrasive wear characteristics of electroless nickel phosphor (Ni-P) coatings on aluminium-alloy substrate LM24 was studied by Rajendran, Sha and Elansezhian (2010). The post treatment consists of heat treatment and followed by lapping procedures. A Plint TE66 micro-abrasion tester with mate material of stainless steel ball was used to evaluate the tribological properties of the coated specimens with static load of 0.5N and speed of 0.1m/s. To induce the abrasive wear, SiC particles were fed between the contact of the specimen and the ball. The wear volume was measured progressively up to 2000 ball-revolutions. The presence of hard  $\text{Ni}_3\text{P}$  particles after heat treatment at  $330^\circ\text{C}$  for one hour has increased the hardness of Ni-P coated specimen from 400Hv to 600Hv. It was found that the wear volume of lapped specimen is higher than the specimen without lapping, although it should be otherwise as far as surface roughness is concerned. They emphasized that this is because the negative effect of the increased surface roughness is less important than the abrasive wear resistance offered by the EN coating. Overall, the Ni-P coated aluminium-alloy exhibited higher wear resistance compared to the bare specimen. The heat treated Ni-P coating showed lower wear resistance compared to the specimen without heat treatment despite having higher hardness value.